

Chromomagnetic and chromoelectric dipole moments of quarks in the reduced 331 model

A. I. Hernández-Juárez* and G. Tavares-Velasco
Facultad de Ciencias Físico Matemáticas, Benemérita Universidad
Autónoma de Puebla, Apartado Postal 1152, Puebla, Puebla, México*

A. Moyotl
Ingeniería en Mecatrónica, Universidad Politécnica de Puebla, Tercer Carril del Ejido Serrano s/n,
San Mateo Cuanalá, Juan C. Bonilla, Puebla, Puebla, México
(Dated: August 12, 2021)

The one-loop contributions to the chromomagnetic dipole moment $\hat{\mu}_t(q^2)$ and electric dipole moment $\hat{d}_t(q^2)$ of the top quark are calculated within the reduced 331 model (RM331) for non-zero q^2 . It is argued that the results are gauge independent and thus represent valid observable quantities. In the RM331 $\hat{\mu}_t(q^2)$ receives new contributions from two heavy gauge bosons Z' and V^\pm and one neutral scalar boson h_2 , along with a new contribution from the standard model Higgs boson via flavor changing neutral currents. The latter, which are also mediated by the Z' gauge boson and the scalar boson h_2 , can give a non-vanishing $\hat{d}_t(q^2)$ provided that there is a CP -violating phase. The analytical results are presented in terms of both Feynman parameter integrals and Passarino-Veltman scalar functions, which are useful to cross-check the numerical results. Both $\hat{\mu}_t(q^2)$ and $\hat{d}_t(q^2)$ are numerically evaluated for parameter values still allowed by the constraints from experimental data. It is found that the new one-loop contributions of the RM331 to the real (imaginary) part of $\hat{\mu}_t(q^2)$ are of the order of 10^{-5} (10^{-6}), which are at least three orders of magnitude smaller than the standard model prediction, but are larger than the predictions of other models of new physics. In the RM331 the dominant contribution arising from the V^\pm gauge boson for $\|q\|$ in the 30-1000 GeV interval and a mass m_V of the order of a few hundreds of GeVs. As for $\hat{d}_t(q^2)$, it receives its largest contribution from h_2 exchange and can reach values of the order of 10^{-19} , which is smaller than the contributions predicted by other standard model extensions.

I. INTRODUCTION

The anomalous magnetic dipole moment (MDM) and the electric dipole moment are among the lepton properties that have stirred more interest in the experimental and theoretical areas. Currently, there is a discrepancy between the theoretical standard model (SM) prediction of the muon anomalous MDM and its experimental measurement, which might be a hint of new physics [1]. On the other hand, any experimental evidence of an electric dipole moment would give a clear signal of new sources of CP violation as the SM contributions are negligibly small. With the advent of the LHC, anomalous contributions to the $\bar{t}tg$ coupling have also become the focus of interest. In analogy with the lepton electromagnetic vertex $\bar{\ell}\ell\gamma$, the anomalous $\bar{q}qg$ coupling can be written as

$$\mathcal{L} = -\frac{1}{2}\bar{q}\sigma^{\mu\nu}\left(\tilde{\mu}_q + i\tilde{d}_q\gamma^5\right)T^a q G_{\mu\nu}^a, \quad (1)$$

where $\tilde{\mu}_q$ is the quark chromomagnetic dipole moment (CMDM) and \tilde{d}_q is the quark chromoelectric dipole moment (CEDM), whereas $G_a^{\mu\nu}$ is the gluon field tensor and T^a are the $SU(3)$ color generators. It is also customary to define the CMDM and CEDM in the dimensionless form [2]

$$\hat{\mu}_q \equiv \frac{m_q}{g_S}\tilde{\mu}_q, \quad (2)$$

$$\hat{d}_q \equiv \frac{m_q}{g_S}\tilde{d}_q. \quad (3)$$

On the experimental side, the search for evidences of the anomalous top quark coupling $\bar{t}tg$ is underway at the LHC [2–4]: the most recent bounds on the top quark CMDM and CEDM were obtained by the CMS collaboration [4, 5],

* alaban7_3@hotmail.com

which managed to improve the previous bounds [2] by one order of magnitude. Thus, one would expect that more tight constraints on $\hat{\mu}_t$ and \hat{d}_t could be set in the near future.

As far as the theoretical predictions are concerned, in the SM the CMDM is induced at the one-loop level or higher orders via electroweak (EW) and QCD contributions, whereas the CEDM can only arise up to the three-loop level [6–8]. The SM contributions to the on-shell $\hat{\mu}_t$ have already been studied in [9–11], and more recently the scenario with an off-shell gluon was studied in [12, 13] to address some ambiguities of previous calculations, particularly about the on-shell CMDM, which is divergent and meaningless in perturbative QCD. Since both the top quark CMDM and CEDM could receive a considerable enhancement from new physics contributions, several calculations have been reported in the literature within the framework of extension theories such as two-Higgs doublet models (THDMs) [14], the four-generation THDM [15], models with a heavy Z' gauge boson [11], little Higgs models [16, 17], the minimal supersymmetric standard model (MSSM) [18], unparticle models [19], vector like multiplet models [20], etc. In this work we are interested in the contributions to the top quark CMDM and CEDM in the reduced 331 model [21].

The study of elementary particle models based on the $SU(3)_L \times U(1)_N$ gauge symmetry dates back to the 1970s, when it was still not clear that Weinberg's $SU(2)_L \times U(1)_Y$ model was the right theory of electroweak interactions [22]. After the discovery of the Z and W gauge bosons, since the electroweak gauge group is embedded into $SU(3)_L \times U(1)_N$, the so called 331 models [23, 24] became serious candidates to extend the SM and explain some issues for which it has no answer, such as the flavor problem and a possible explanation for the large splitting between the mass of the top quark and those of the remaining fermions. Several realizations of the 331 model have been proposed in the literature, which predict new fermions, gauge bosons and scalar bosons, so their phenomenologies have been considerably studied [25–32].

The minimal 331 model [23, 24] requires a very large scalar sector, which introduces three scalar triplets to give masses to the new heavy gauge bosons and one scalar sextet to endow the leptons with small masses. The complexity of this model has led to the appearance of alternative 331 models aimed to economize the scalar sector. In particular, the reduced 331 model (RM331) [21] only requires two scalar triplets, thereby being considerably simpler than the minimal version [33, 34]. In the RM331, the physical scalar states obtained after the symmetry breaking are two neutral scalar bosons only, with the lightest one being identified with the SM Higgs boson [35], and a doubly charged one. Unlike other 331 models, no singly charged scalar boson arises in the RM331 [36–38]. In the gauge sector, there are one new neutral gauge boson Z' , a new pair of singly charged gauge bosons V^\pm , and a pair of doubly charged gauge bosons $U^{\pm\pm}$. Like other 331 models, the RM331 also predicts three new exotic quarks. The original RM331 is strongly disfavored by experimental data [39], though it would still be allowed as long as left-handed quarks are introduced via a particular $SU(3)_L \times U(1)_N$ representation [40, 41], which in fact would give rise to flavor changing neutral current (FCNC) effects.

The contributions to the electron and muon anomalous MDM have been already studied in the RM331 [26] within another 331 realization [42]. As for the CMDM of quarks, there is only a previous calculation in the context of an old version of the 331 model [9], though such a calculation is limited to the on-shell case. However, since the on-shell CMDM is infrared divergent in the SM [12], a calculation of the off-shell CMDM is mandatory. To our knowledge there is no calculation of the off-shell CMDM of quarks, let alone their off-shell CEDM, in 331 models. Furthermore, in the model studied in [9], the new contributions only arise in the gauge sector, whereas in the RM331 there are additional contributions from the neutral scalar bosons, which are absent in other 331 models.

In this work we present a study on the contributions of the RM331 to the off-shell CMDM and CEDM of the top quark. Our manuscript is organized as follows. In Section II we present a brief description of the RM331, with the Feynman rules necessary for our calculation being presented in Appendix A. The analytical calculation of the new contributions to the dipole form factors of the $\bar{t}tg$ vertex are presented in Sec. III; our results in terms of Feynman parameter integrals and Passarino-Veltman scalar functions are presented in Appendix B. Section IV is devoted to a review of the current constraints on the parameter space of the model and the numerical analysis of the off-shell CMDM and CEDM of the top quark. Finally, in Sec. V the conclusions and outlook are presented.

II. BRIEF OUTLINE OF THE RM331

We will describe briefly the main features of each sector of the RM331, focusing only on those details relevant to our calculation.

A. Scalar and gauge boson eigenstates

As far as the scalar sector is concerned, the scalar potential is given by

$$V(\chi, \rho) = \mu_1^2 \rho^\dagger \rho + \mu_2^2 \chi^\dagger \chi + \lambda_1 (\rho^\dagger \rho)^2 + \lambda_2 (\chi^\dagger \chi)^2 + \lambda_3 (\rho^\dagger \rho) (\chi^\dagger \chi) + \lambda_4 (\rho^\dagger \chi) (\chi^\dagger \rho), \quad (4)$$

where the scalar triplets transform as $\rho = (\rho^+, \rho^0, \rho^{++})^T \sim (1, 3, 1)$ and $\chi = (\chi^-, \chi^{--}, \chi^0)^T \sim (1, 3, -1)$. To induce the spontaneous symmetry breaking (SSB), the neutral scalar bosons ρ^0 and χ^0 develop non-zero vacuum expectation values (VEVs) under the shifting of the fields as

$$\rho^0, \chi^0 \rightarrow \frac{1}{\sqrt{2}} (v_{\rho, \chi} + R_{\rho, \chi} + iI_{\rho, \chi}), \quad (5)$$

which leads to the following constraints

$$\begin{aligned} \mu_1^2 + \lambda_1 v_\rho^2 + \frac{\lambda_3 v_\chi^2}{2} &= 0, \\ \mu_2^2 + \lambda_2 v_\chi^2 + \frac{\lambda_3 v_\rho^2}{2} &= 0. \end{aligned}$$

The $SU(3)_C \times SU(3)_L \times U(1)_N$ breaks down into the SM gauge group following the pattern

$$SU(3)_L \times U(1)_N \xrightarrow{\langle \chi^0 \rangle} SU(2)_L \times U(1)_Y \xrightarrow{\langle \rho^0 \rangle} U(1)_{\text{EM}}, \quad (6)$$

where v_ρ can be identified with the SM Higgs VEV v . The left-over of SSB are two neutral scalar bosons and a pair of doubly charged ones $h^{\pm\pm}$ as explained below.

The mass matrix of the neutral scalar bosons in the (R_χ, R_ρ) basis is

$$\mathbf{m}_0^2 = \frac{v_\chi^2}{2} \begin{pmatrix} 2\lambda_2 & \lambda_3 t \\ \lambda_3 t & 2\lambda_1 t^2 \end{pmatrix},$$

where $t = v_\rho/v_\chi$. After diagonalization, the mass eigenstates in the limit $v_\chi \gg v_\rho$ are

$$h_1 = c_\beta R_\rho - s_\beta R_\chi, \quad h_2 = c_\beta R_\chi + s_\beta R_\rho, \quad (7)$$

with masses

$$m_{h_1}^2 = \left(\lambda_1 - \frac{\lambda_3^2}{4\lambda_2} \right) v_\rho^2, \quad (8)$$

$$m_{h_2}^2 = \lambda_2 v_\chi^2 + \frac{\lambda_3^2}{4\lambda_2} v_\rho^2, \quad (9)$$

where $\lambda_1, \lambda_2 > 0$ and $c_\beta \equiv \cos \beta \approx 1 - \lambda_3^2 v_\rho^2 / (8\lambda_2^2 v_\chi^2)$. The SM Higgs boson h can be recovered in the $s_\beta \rightarrow 0$ limit, thus h_1 must be identified with the Higgs boson discovered at the LHC. Since $m_h \simeq 125$ GeV, from Eq. (8) we obtain the relation $\lambda_1 - \lambda_3^2 / (4\lambda_2) \approx 0.26$ [1]. In the case $\lambda_2, \lambda_2 < 1$, and $\lambda_3 < \lambda_2$ we obtain $m_{h_1}^2 = \lambda_1 v_\rho^2$, which recovers the SM case and thus $\lambda_1 \approx 0.26$.

In the gauge sector there are two new singly charged gauge bosons V^\pm , two doubly charged gauge bosons $U^{\pm\pm}$ and a neutral gauge bosons Z' . They acquire their masses as follows. The would-be Goldstone bosons χ^\pm are eaten by the singly charged gauge bosons, whereas a linear combination of the doubly charged would-be Goldstone bosons $\rho^{\pm\pm}$ and $\chi^{\pm\pm}$ are absorbed by the doubly charged gauge boson $U^{\pm\pm}$. Also, the orthogonal combination of $\rho^{\pm\pm}$ and $\chi^{\pm\pm}$ gives rise to a physical doubly charged scalar boson pair $h^{\pm\pm}$. Finally, the would-be Goldstone boson I_χ becomes the longitudinal components of the Z' gauge boson. Thus, the masses of the new gauge bosons at leading order at v_χ are [43]

$$m_{Z'}^2 = \frac{g^2 c_W^2}{3(1 - 4s_W^2)} v_\chi^2, \quad (10)$$

$$m_{V^\pm}^2 = \frac{g^2}{4} v_\chi^2, \quad (11)$$

$$m_{U^{\pm\pm}}^2 = \frac{g^2}{4} (v_\rho^2 + v_\chi^2). \quad (12)$$

As far as the SM gauge bosons are concerned, the would-be Goldstone bosons ρ^\pm and I_ρ endow with masses the Z and W^\pm gauge bosons, respectively.

B. Gauge and scalar boson couplings to the top quark

The number of new fermions necessary to fill out the $SU(3)_L \times U(1)_N$ multiplets as well as their quantum numbers depend on the particular 331 model version. There are no new leptons in the RM331, but a new quark is required for each quark triplet. They transform as

$$Q_{iL} = \begin{pmatrix} d_i \\ -u_i \\ J_i \end{pmatrix}_L \sim (3, 3^*, -1/3), \quad i = 1, 2, \quad Q_{3L} = \begin{pmatrix} u_3 \\ d_3 \\ J_3 \end{pmatrix}_L \sim (3, 3, +2/3),$$

with the numbers between parentheses representing the field transformations under the $SU(3)_C \times SU(3)_L \times U(1)_N$ gauge group, whereas J_1, J_2 and J_3 are the new exotic quarks with electric charges $Q_{J_{1,2}} = -4/3e$ and $Q_{J_3} = 5/3e$. Under this representation the theory is anomaly free [40].

1. Charged currents

In the quark sector, the charged currents relevant for our calculation are given by the following Lagrangian

$$\mathcal{L}_q^{CC} = \frac{g}{\sqrt{2}} \bar{u}_L V_{CKM}^q \gamma^\mu d_L W_\mu^+ + \frac{g}{\sqrt{2}} \bar{J}_{3L} \gamma^\mu (V_L^u)_{3a} u_{aL} V_\mu^+ + \frac{g}{\sqrt{2}} \bar{u}_L (V_L^{u\dagger})_{li} \gamma^\mu J_{iL} U_\mu^{++} + \text{H.c.},$$

where the family index a runs over 1, 2 and 3, whereas i and l run over 1 and 2. Also $V_{CKM}^q = V_L^{u\dagger} V_L^d$ stands for the Cabibbo-Kobayashi-Maskawa matrix, with the mixing matrices V_L^u (V_L^d) transforming the left-handed up (down) quarks flavor eigenstates into their mass eigenstates. It is assumed that the new quarks are given in their diagonal basis. Note that the doubly charged gauge boson $U^{\pm\pm}$ does not couple to the top quark.

2. FCNC currents

Since the Z' gauge boson couplings to the quarks are non-universal, flavor changing neutral currents (FCNCs) are induced at the tree level. The corresponding Lagrangian for the up quark sector reads

$$\mathcal{L}_{Z'}^{FCNC} = \frac{g}{2c_W \sqrt{3(1-4s_W^2)}} \left(\sum_{a=1}^3 (\bar{u}'_{aL} \gamma^\mu (1-2s_W^2) u'_{aL}) + \bar{u}'_{3L} \gamma^\mu (2s_W^2) u'_{3L} \right) Z'_\mu, \quad (13)$$

where the up quarks u' are in the flavor basis. It is evident that the above Lagrangian induces FCNC at the tree level after the rotation to the mass eigenstate basis.

On the other hand, the interactions between up quarks and the neutral scalar bosons arise from the lagrangian

$$\mathcal{L}_S = \sum_{i,j=1}^3 \bar{u}'_{iL} \Gamma_{1ij}^u u'_{jR} h_1 + \bar{u}'_{iL} \Gamma_{2ij}^u u'_{jR} h_2 + \text{H.c.}, \quad (14)$$

where u' is an up quark triplet $u'^T = (u', c', t')$ and

$$\Gamma_1^u = \frac{c_\beta}{v_\rho} \mathbf{m}^u - \frac{s_\beta}{v_\chi} \begin{pmatrix} 0 & 0 & 0 \\ 0 & 0 & 0 \\ m_{31}^u & m_{32}^u & m_{33}^u \end{pmatrix},$$

$$\Gamma_2^u = \frac{s_\beta}{v_\rho} \mathbf{m}^u + \frac{c_\beta}{v_\chi} \begin{pmatrix} 0 & 0 & 0 \\ 0 & 0 & 0 \\ m_{31}^u & m_{32}^u & m_{33}^u \end{pmatrix},$$

with \mathbf{m}^u being the quark mass matrix in the flavor basis [40]. After rotating to the mass eigenstate basis, only the terms proportional to \mathbf{m}^u are diagonalized, whereas the remaining term gives rise to FCNC couplings, which can be written as

$$\mathcal{L}_S^{FCNC} = \sum_{i,j=1}^3 (-s_\beta \bar{u}_{iL} \eta_{ij}^u u_{jR} h_1 + c_\beta \bar{u}_{iL} \eta_{ij}^u u_{jR} h_2) + \text{H.c.}, \quad (15)$$

where

$$\eta^u = \mathbf{V}_L^u \begin{pmatrix} 0 & 0 & 0 \\ 0 & 0 & 0 \\ \frac{m_{31}^u}{v_\chi} & \frac{m_{32}^u}{v_\chi} & \frac{m_{33}^u}{v_\chi} \end{pmatrix} (\mathbf{V}_R^u)^\dagger.$$

Through the parametrization given in [44] for the $\mathbf{V}_{L,R}^{u,d}$ mixing matrices it is possible to obtain numerical values for the entries of the $\eta^{u,d}$ matrix. Under this framework $m_{31}^u = 0$, $m_{32}^u = 0$, and $m_{33}^u = m_t$.

III. CMDM AND CEDM OF THE TOP QUARK IN THE RM331

Apart from the pure SM contributions, at the one-loop level there are new contributions to the CMDM of the top quark arising in both the gauge and scalar sectors of the RM331. The corresponding Feynman diagrams are depicted in Fig. 1. In the gauge sector the new contributions arise from the neutral Z' gauge boson, which are induced by both diagonal and non-diagonal couplings. There are also a new contribution from the singly-charged gauge boson V^\pm , which is accompanied by the new exotic quark J_3 . As already noted, the doubly-charged gauge boson $U^{\pm\pm}$ does not couple to the top quark, thus there is no contribution from this gauge boson to the top quark CMDM and CEDM. As for the scalar sector, there are new contributions from the neutral scalar bosons h_1 and h_2 , which in fact are the novel contributions from the RM331 as they are absent in other 331 model versions. The SM-like Higgs boson h_1 yields new contributions arising from its FCNC couplings, which are induced at the tree-level, but also from its diagonal coupling, which has a small deviation from its SM value. As for the new Higgs boson h_2 , it also contributes via both diagonal and non-diagonal couplings. We would like to point out that such scalar contributions are absent in the 331 model studied in Ref. [9], where the on-shell CMDM of the top quark was calculated. Even more, as long as complex FCNC couplings are considered, there are non-vanishing contributions to the CEDM. This class of contributions has also not been studied before in the context of 331 models.

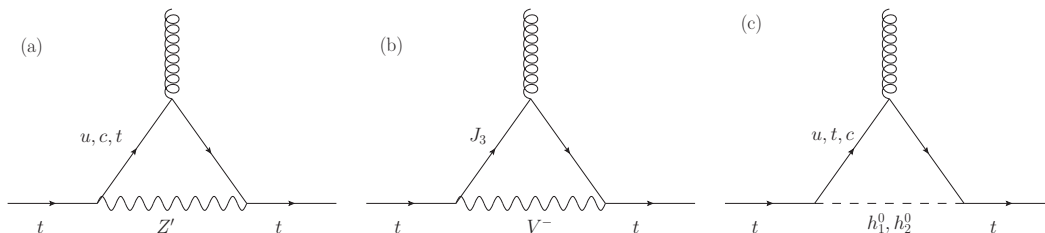


FIG. 1. New one-loop contributions of the RM331 to the CMDM and CEDM of the top quark in the unitary gauge. In the conventional linear R_ξ gauge there are additional Feynman diagrams where the gauge bosons are replaced by their associated Goldstone bosons.

We are interested in the off-shell CMDM and CEDM of the top quark. Since off-shell Green functions are not associated with an S -matrix element, they can be plagued by pathologies such as being gauge non-invariant, gauge dependent, ultraviolet divergent, etc. Along these lines, the pinch technique (PT) was meant to provide a systematic approach to construct well-behaved Green functions [45], out of which valid observable quantities can be extracted. It was later found that there is an equivalence at least at the one-loop level between the results found via the PT and those obtained through the background field method (BFM) via the Feynman gauge [46]. This provides a straightforward computational method to obtain gauge independent Green functions. It is thus necessary to verify whether the RM331 contributions to the CMDM and CEDM of quarks are gauge independent for $q^2 \neq 0$. Nevertheless, we note that from the Feynman diagrams of Fig. 1, the gauge parameter ξ only enters into the amplitudes of the Feynman diagrams (a) and (b) via the propagators of the gauge bosons and their associated would-be Goldstone bosons. Those kind of diagrams have an amplitude that shares the same structure to those mediated by the electroweak gauge bosons Z and W in the SM, which are known to yield a gauge independent contribution to the CMDM for an off-shell gluon when the contribution of their associated would-be Goldstone bosons are added up. See for instance Ref. [12], where we calculate the electroweak contribution to the CMDM of quarks in the conventional linear R_ξ gauge and verify that the gauge parameter ξ drops out. Furthermore, the dipole form factors cannot receive contributions from self-energy diagrams, which are required to cancel gauge dependent terms appearing in the monopolar terms via the PT approach. Thus both the CMDM and CEDM must be gauge independent for an off-shell gluon and thus valid observable quantities.

Below we present the analytical results of our calculation in a model-independent way, out of which the results for the RM331 and other SM extensions would follow easily. The corresponding coupling constants for the RM331 are presented in Appendix A. For the loop integration we used the Passarino-Veltman reduction method and for completeness our calculation was also performed by Feynman parametrization via the unitary gauge, which provides alternative expressions to cross-check the numerical results. The Dirac algebra and the Passarino-Veltman reduction were done in Mathematica with the help of FeynCalc [47] and Package-X [48].

A. New gauge boson contributions

We first consider the generic contribution of a new gauge boson V with the following interaction to the quarks

$$\mathcal{L}^{Vqq'} = \frac{g}{c_W} \bar{q} \left(g_V^{Vqq'} - g_A^{Vqq'} \gamma^5 \right) \gamma_\mu q' V^\mu + \text{H.c.}, \quad (16)$$

where the coupling constants $g_{V,A}^{Vqq'}$ are taken in general as complex quantities. By hermicity they should obey $g_{V,A}^{Vqq'} = g_{V,A}^{Vq'q*}$.

The above interaction gives rise to a new contribution to the quark CMDM and CEDM via a Feynman diagram similar to that of Fig. 1(a). The corresponding contribution to the quark CMDM can be written as

$$\hat{\mu}_q^V(q^2) = \frac{G_F m_W^2}{2\sqrt{2}\pi^2 r_V^2 c_W^2} \sum_{q'} \left| g_V^{Vqq'} \right|^2 \mathcal{V}_{qq'}^V(q^2) + \left(\begin{array}{l} g_V^{Vqq'} \rightarrow g_A^{Vqq'} \\ m'_q \rightarrow -m'_q \end{array} \right), \quad (17)$$

where we introduced the auxiliary variable $r_a = m_a/m_q$ and the $\mathcal{V}_{qq'}^V(q^2)$ function is presented in Appendix B in terms of Feynman parameter integrals and Passarino-Veltman scalar functions. The second term of the right-hand side stands for the first term with the indicated replacements. As for the contribution to the quark CEDM, it can arise as long as there are flavor changing complex couplings and is given by

$$\hat{d}_q^V(q^2) = \frac{G_F m_W^2}{\sqrt{2}\pi^2 r_V^2 c_W^2} \sum_{q'} \text{Im} \left(g_V^{Vqq'} g_A^{Vqq'*} \right) \tilde{\mathcal{D}}_{qq'}^V(q^2), \quad (18)$$

where again the $\mathcal{D}_{qq'}^V(q^2)$ function is presented in Appendix B.

From Eqs. (17) y (18) we can obtain straightforwardly the contributions to the quark CMDM and CEDM of the neutral gauge boson Z' and the singly charged gauge boson V^\pm after replacing the coupling constants and the gauge boson masses.

B. New scalar boson contributions

Following the same approach as above, we now present the generic contribution to the quark CMDM and CEDM arising from FCNC mediated by a new scalar boson S , which arise from the Feynman diagram of Fig 1(c). We consider an interaction of the form

$$\mathcal{L}^{Sqq'} = -\frac{g}{2} \bar{q} \left(G_S^{Sqq'} + G_P^{Sqq'} \gamma^5 \right) q' S + \text{H.c.} \quad (19)$$

The above scalar interaction leads to the following contribution to the quark CMDM

$$\hat{\mu}_q^S(q^2) = -\frac{G_F m_W^2}{8\sqrt{2}\pi^2} \sum_{q'} \left| G_P^{Sqq'} \right|^2 \mathcal{P}_{qq'}^S(q^2) + \left(\begin{array}{l} G_P^{Sqq'} \rightarrow G_S^{Sqq'} \\ m'_q \rightarrow -m'_q \end{array} \right), \quad (20)$$

whereas the corresponding contribution to the quark CEDM is given by

$$\hat{d}_q^S(q^2) = \frac{G_F m_W^2}{4\sqrt{2}\pi^2} \sum_{q'} \text{Im} \left(G_S^{Sqq'} G_P^{Sqq'*} \right) \tilde{\mathcal{D}}_{qq'}^S(q^2), \quad (21)$$

where the $\mathcal{P}_{qq'}^S(q^2)$ and $\tilde{\mathcal{D}}_{qq'}^S(q^2)$ functions are presented in Appendix B.

From the above expression we can obtain the contribution of the new scalar Higgs boson of the RM331 as well as the contribution of the SM Higgs boson, which in the RM331 has tree-level FCNC couplings.

IV. NUMERICAL ANALYSIS AND DISCUSSION

We now turn to the numerical analysis. The coupling constants that enter into the Feynman rules and are necessary to evaluate the CMDM and CEDM of the top quark [c.f. Eqs. (16) through (21)] are presented in Tables III and IV of Appendix A. We note that these couplings depend on several free parameters, such as the mass parameter m_{33}^u , the VEV v_χ , the parameters of the scalar potential λ_2 and λ_3 , as well as the entries of the matrices \mathbf{V}_L^u , \mathbf{K}_L and $\boldsymbol{\eta}^u$. To obtain an estimate of the contributions of the RM331 to the CMDM and CEDM of the top quark we need to discuss the most up-to-date constraints on these parameters from current experimental data.

A. Constraints on the parameter space

1. Heavy particle masses

As already mentioned, the mass parameter m_{33}^u can be identified with the top quark mass [40], whereas the VEV v_χ determines the masses of the heavy gauge bosons and the heavy quark J_3 . As for the mass of the new scalar boson m_{h_2} , it is determined by the parameters λ_2 and λ_3 , along with the VEV v_χ , which also determine the mixing angle s_β .

We will first discuss the current indirect constraints on the heavy neutral gauge boson masses. From the muon $g-2$ discrepancy, the following constraint was obtained $v_\chi \gtrsim 2$ TeV [41], from which bounds on the heavy gauge boson masses follow. Nevertheless, there are also indirect constraints obtained through the experimental data on $B^0 - \bar{B}^0$ oscillations. The RM331 contribution to Δm_B arises from FCNC couplings mediated by the Z' gauge boson and the h_1 and h_2 scalar bosons [40, 43], then using the parametrization of [44], the experimental limit on Δm_B leads to the following bounds $m_{Z'} \gtrsim 3.3$ TeV, $m_{V^\pm} \gtrsim 0.33$ TeV and $m_{h_2} \gtrsim 0.34$ TeV [40]. Similar limits have been imposed using the mass difference of the $K^0 - \bar{K}^0$ and $D - \bar{D}^0$ systems [43]. On the other hand, the current experimental bounds on the masses of new neutral and charged heavy gauge bosons from collider searches are model dependent [1]. At the LHC, the ATLAS and CMS Collaborations have searched for an extra charged gauge boson W' at $\sqrt{s} = 13$ TeV via the decay modes $W' \rightarrow \ell\nu_\ell$ [49, 50] and $W' \rightarrow qq'$. The most stringent bounds are obtained for a W' gauge boson with SM couplings (sequential SM). The respective lower bounds on $m_{W'}$ are 6.0 TeV (5.1 TeV) for the $W' \rightarrow e\nu_e$ ($W' \rightarrow \mu\nu_\mu$) decay channel, whereas for the decay $W' \rightarrow qq'$ the corresponding bound is less stringent, of the order of 4 TeV [51, 52]. As far as an extra neutral gauge boson Z' is concerned, the search at the LHC at $\sqrt{s} = 13$ TeV via its decays into a lepton pair has been useful to impose the lower limit $m_{Z'} \geq 4.5, 5$ TeV for a Z' gauge boson model arising in the sequential SM and in an E_6 -motivated Grand Unification model [53, 54]. Along these lines, it has been pointed out recently that the LHC might be able to constrain the mass of the heavy Z' boson up to the 5 TeV level in several 331 models [55–57]. Although these bounds are model dependent and relies on several assumptions, if we consider the conservative value of 5 TeV for the gauge boson masses we obtain a lower constraint on v_χ of the order of 10 TeV. Thus, we will use this value in our analysis to be consistent with experimental constraints and limits from FCNC couplings.

As far as direct constraints on the mass of exotic quarks are concerned, the ATLAS and CMS Collaborations have used the $\sqrt{s} = 13$ TeV data to search for vector-like quarks with electric charge of $5/3$ via its decay into a top quark and a W gauge boson, with the final state consisting of a single charged lepton (muon or electron), missing transverse momentum, and several jets. A mass exclusion limit up to 1.6 TeV is obtained depending on the properties of the vector-like quark [58–60]. We will thus use $m_{J_3} = 2$ TeV to be consistent with the experimental bound.

2. Mixing angle s_β and parameters $\lambda_{2,3}$

According to Eq. (8) the mass of the SM-like Higgs boson receives new corrections through the λ_2 and λ_3 parameters. As discussed above, the SM case is recovered when $\lambda_1 \approx 0.26$ and $\lambda_3 < \lambda_2 < 1$, thus the new corrections to m_{h_1} must lie within the experimental error of the SM Higgs boson mass $m_h = 125.10 \pm 0.14$ GeV [1]. This allows one to constrain the λ_2 and λ_3 parameters, which in turn translates into constraints on s_β and m_{h_2} once the v_χ value is fixed. Again we take a conservative approach and only consider the experimental uncertainty in the Higgs boson mass, whereas theoretical uncertainties from higher order corrections are not taken into account. We observe in Fig. 2 the allowed regions in the planes λ_2 vs λ_3 and s_β vs m_{h_2} consistent with the experimental error of the Higgs boson mass at 95% C.L. We note that for a given λ_2 , λ_3 must be about one order of magnitude below. In our calculation we use $\lambda_2 = 0.9$ and $\lambda_3 = 0.06$, though there is no great sensitivity of the top quark CMDM and CEDM to mild changes in the values of these parameters. In addition, we find that values ranging from 0.002 to 0.013 are allowed

for s_β provided that $v_\chi \geq 10$ TeV and $m_{h_2} \gtrsim 300$ GeV, which is consistent with recent searches for new neutral scalar bosons at the LHC [1].

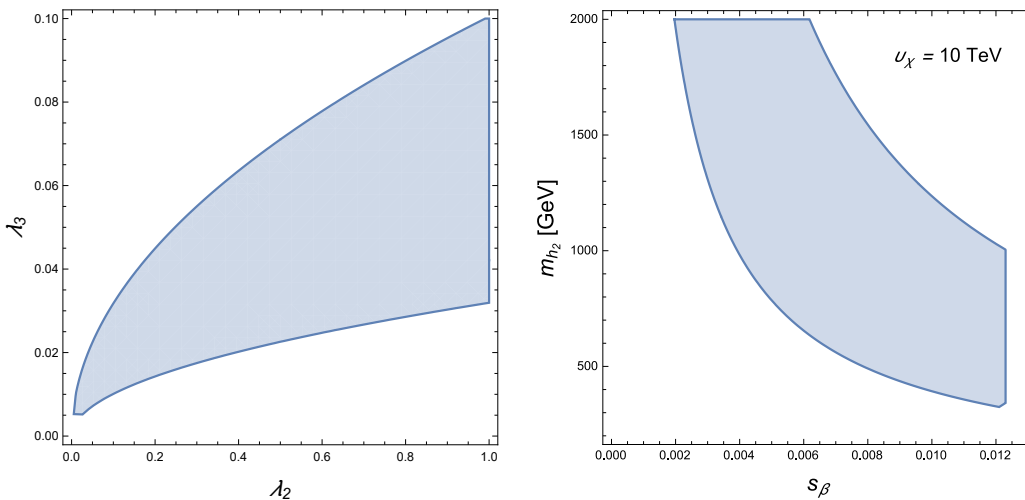


FIG. 2. Allowed areas in the planes λ_3 vs λ_2 and s_β vs m_{h_2} in agreement with the experimental error of the Higgs boson mass $m_h = 125.10 \pm 0.14$ GeV [1] at 95% C.L. We consider $\lambda_1 \approx 0.26$ and $\lambda_3 < \lambda_2 < 1$, which yield the SM limit.

3. Mixing matrices

As for the mixing matrices, we can obtain the absolute values for the entries of the matrices \mathbf{V}_L^u , \mathbf{K}_L and $\boldsymbol{\eta}^u$. The entries of the last matrix are given in terms of v_χ , s_β and the m_{ij}^q matrix elements and their values are obtained following the parametrization used in [44]. In general \mathbf{K}_L and $\boldsymbol{\eta}^u$ are in terms of the entries of \mathbf{V}_L^u and \mathbf{V}_R^u , the complex matrices that diagonalize the mass matrices of up quarks. These matrices can be assumed to be triangular, then using the experimental data on quark masses and the mixing angles it is possible to obtain values of their entries [61]. It is also assumed that the only non-negligible mixing is that arising between the third and second fermion families. Furthermore, since the CP violation phases are expected to be very small, we take a conservative approach and assume complex phases of the order of 10^{-3} .

We present in Table I a summary of the numerical values we will use in our numerical evaluation.

TABLE I. Values of the parameters used in our evaluation of the CMDM and CEDM of the top quark in the RM331. For the entries of the matrices \mathbf{V}_L^u , \mathbf{K}_L and $\boldsymbol{\eta}^u$ we use the values obtained in [40] using the parametrization of [44], where the mass parameter m_{33}^u is identified with the top quark mass. We use λ_2 and λ_3 values allowed by the experimental error in the Higgs boson mass and also assume that the only non-negligible mixing is that arising between the third and second fermion families.

Parameter	Value
$ (K_L)_{tc} $	6.4×10^{-4}
$ V_{33}^u $	1
$ \eta_{tc}^u $	6.4×10^{-4}
$ \eta_{ct}^u $	4.62×10^{-6}
m_{33}^u	m_t
v_χ	10 TeV
s_β	10^{-2}
m_{h_2}	300 GeV
$\phi_{\eta_{tc}^u}, \phi_{\eta_{ct}^u}$	10^{-3}

B. Top quark CMDM

As already mentioned, in the RM331 there are new contributions to the off-shell top quark CMDM $\mu_t(q^2)$ arising from the heavy gauge bosons Z' and V^\pm as well as the neutral scalar bosons h_1 and h_2 . Below we will use the notation A_{BC} for the contribution of particle A due to the ABC coupling. Thus, for instance Z'_{tc} will denote the contribution of the loop with the Z' gauge boson due to the $Z'tc$ coupling. Since we would like to assess the magnitude of the new physics contributions to $\hat{\mu}_t(q^2)$, we will extract from our calculation the pure SM contributions. Thus, apart from the contribution due to the tree-level FCNCs of the SM-like Higgs boson h_1 , we only consider the contribution arising from the small deviation of the diagonal coupling h_1tt from the SM htt coupling. This contribution will be denoted by δh_{1tt} .

We will examine the behavior of the CMDM of the top quark as a function of $\|q\| \equiv \sqrt{|q^2|}$, where q is the gluon four-momentum. In the left plot of Fig. 3 we show the real part of the partial contributions to $\hat{\mu}_t(q^2)$ as a function of $\|q\|$ for the parameter values of Table I, whereas the real and imaginary parts of the total contribution are shown in the right plot. In general there is little dependence of $\text{Re}[\hat{\mu}_t(q^2)]$ on $\|q\|$, except for the δh_{1tt} , h_{2tt} and h_{2tc} contributions, which have a change sign. We also note that the $V_{tJ_3}^\pm$ contribution is the largest one, whereas the remaining contributions are negligible, with the h_{1tc} contribution being the smallest one. Thus the curve for the real part of the total contribution seems to overlap with that of the $V_{tJ_3}^\pm$ contribution, though the former shows a small peak at $\|q\| \simeq 2m_t$. This can be explained by the peak appearing in the δh_{1tt} contribution, which can be as large as the $V_{tJ_3}^\pm$ contribution for $\|q\| \simeq 2m_t$. We conclude that $\hat{\mu}_t(q^2)$ can have a real part of the order of 10^{-5} .

As far as the imaginary parts of the partial contributions to $\hat{\mu}_t(q^2)$, they are several orders of magnitude smaller than the corresponding real parts. As observed in the right plot of Fig. 3, the imaginary part of the total contribution is negligible for $\|q\| \leq 2m_t$, but increases up to about 10^{-6} around $\|q\| = 400$ GeV, where it starts to decrease up to one order of magnitude as $\|q\|$ increases up to 1 TeV.

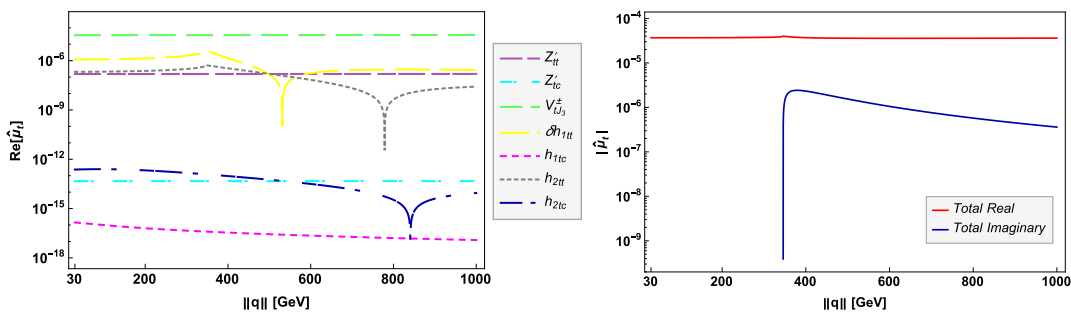


FIG. 3. Real part of the partial contributions of the RM331 to the top quark CMDM (left plot) as a function of $\|q\| \equiv \sqrt{|q^2|}$ for the parameter values of Table I. The real and imaginary parts of the total contribution are shown in the right plot.

Analogue plots to those of Fig. 3, but now for the behavior of $\hat{\mu}_t(q^2)$ as a function of v_χ for $\|q\| = 500$ GeV and the parameter values of Table I, are shown in Fig. 4. In this case we observe that the real parts of the partial contributions to $\hat{\mu}_t(q^2)$ show a variation of about one order of magnitude when v_χ increases from 10 TeV to 20 TeV. As already noted, the $V_{tJ_3}^\pm$ contribution yields the bulk of the total contribution to $\hat{\mu}_t$, whose imaginary part is slightly larger than its real part. Therefore both real and imaginary contributions of the RM331 to the top quark CMDM can be as large as 10^{-5} .

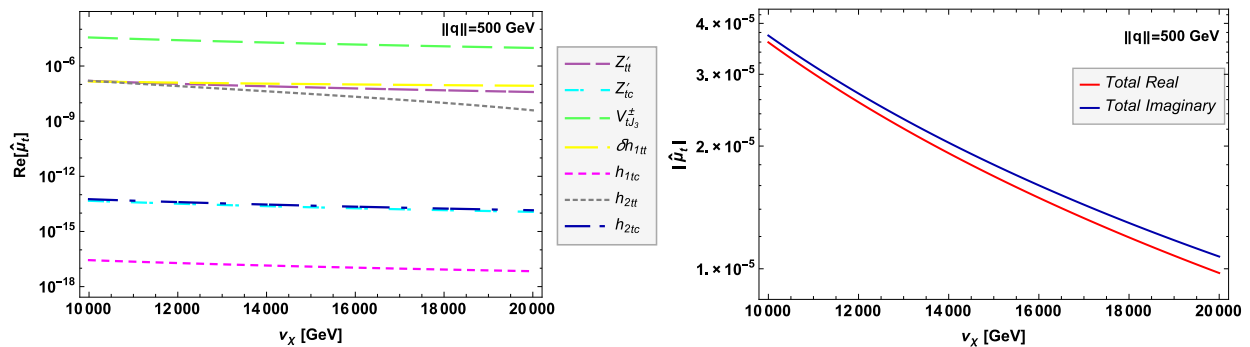


FIG. 4. The shares as in Fig. 3 but for the contributions of the RM331 to the top quark CMDM as functions of v_χ for $\|q\|=500$ GeV. For the remaining parameters we use the values of Table I.

In summary, for $v_\chi \geq 10$ TeV the real part of the the RM331 new contribution to $\hat{\mu}_t(q^2)$ would be three orders of magnitude smaller than the real part of the SM electroweak contribution [12], whereas its imaginary part can be as large than its real part. In general there is no appreciable variation in the magnitude of $\hat{\mu}_t$ for mild changes in the parameters of Table I. Although $\hat{\mu}_t(q^2)$ can be of similar size than the SM electroweak prediction for $v_\chi \leq 10$ TeV, such values are disfavored by the current constrains on the heavy gauge bosons masses. Finally, we note that the RM331 can give a contribution larger than the ones predicted by other extension models where a new neutral Z gauge boson is predicted [11]. The real and imaginary parts of the top quark CMDM are of order $10^{-6} - 10^{-7}$ and $10^{-10} - 10^{-11}$ respectively in such models.

C. Top quark CEDM

A potential new source of CP violation can arise in the RM331 through the FCNC couplings mediated by the neutral scalar bosons, which are proportional to the entries of the non-symmetric complex mixing matrix η^u [40], thereby allowing the presence of a non-zero CEDM, which is absent in other 331 models. Thus, it is a novel prediction of the RM331.

There are only two partial contributions to the top quark CEDM in the RM331, thus we only analyze the behavior of the total contribution. We show in Fig. 5 the contour lines of the real part (left plot) and the imaginary part (right plot) of $d_t(q^2)$ in the v_χ vs $\|q\|$ plane for the parameter values of Table I. We have found that the new scalar boson h_2 yields the dominant contribution to $d_t(q^2)$, whose real (imaginary) part can be as large as 10^{-19} (10^{-20}), whereas the contribution from the h_1 scalar boson is three or more orders of magnitude below. We also observe that the real part of $d_t(q^2)$ decreases as v_χ and $\|q\|$ increase, while the imaginary part remains almost constant. For $\|q\| \geq 600$ GeV, the RM331 contribution to the CEDM of the top quark is expected to be below the 10^{-20} level, which seems to be much smaller than the values predicted in other extension models [11], where the real and imaginary parts are of order $10^{-7} - 10^{-8}$ and $10^{-12} - 10^{-13}$ respectively. In the range $2 \text{ TeV} \leq v_\chi \lesssim 10 \text{ TeV}$ our results for $d_t(q^2)$ are enhanced by one order of magnitude, but as already noted, this interval is disfavored by current constraints.

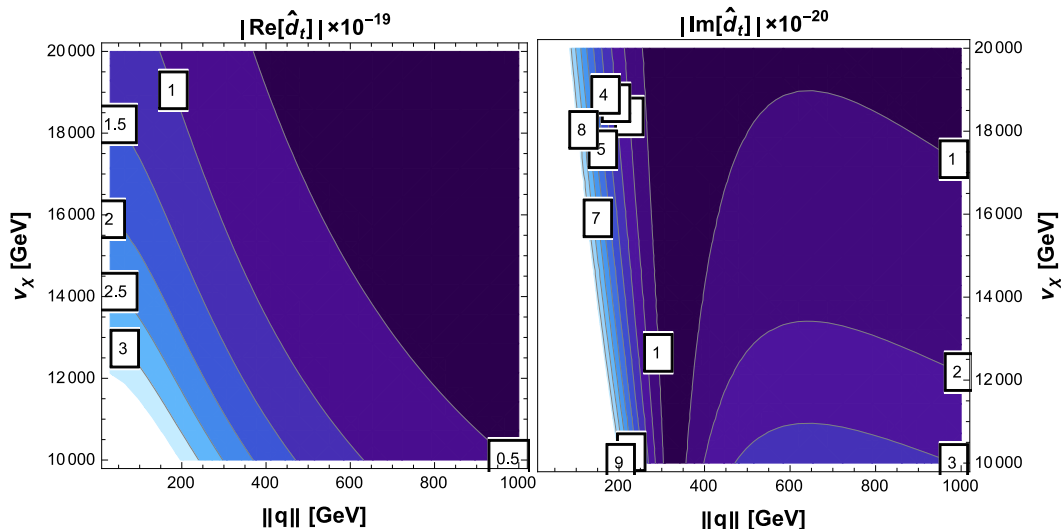


FIG. 5. Real part (left plot) and imaginary part (right plot) of the total contribution to the CEDM of the top quark in the RM331 in the plane v_χ vs $\|q\|$. We use the parameter values of Table I.

For comparison, a compilation of the predictions of several extension models of the top quark CMDM and CEDM for $q^2 = 0$ is presented in Table II. We would like to stress that to our knowledge there is no previous estimate of the top quark CEDM in 331 models. We also note that though these values seem to be much larger than the results obtained for $q^2 \neq 0$ in the RM331, the dipole form factors are expected to decrease as q^2 increases. Such a behavior is indeed observed in the SM case [12], where the magnitude of \hat{a}_t decreases as $\|q\|$ increases.

TABLE II. Predictions of the CMDM and CEDM of the top quark in several extension models at $q^2 = 0$.

Model	\hat{a}_t	\hat{d}_t
SM	10^{-2} [12, 13]	
THDMs	$10^{-3}-10^{-1}$ [14]	10^{-5} [14, 62]
4GTHDM	$10^{-2}-10^{-1}$ [15]	$10^{-5}-10^{-4}$ [15]
331	10^{-5} [9]	
Technicolor	10^{-2} [9]	
Extra dimensions	10^{-3} [9]	
Little Higgs model	10^{-6} [17]	
MSSM	10^{-1} [18]	$10^{-5} - 10^{-4}$ [63]
Unparticle model	10^{-2} [19]	
Vector-like multiplets		10^{-4} [20]

V. CONCLUSIONS

We have presented a calculation of the one-loop contributions to the CMDM and CEDM, $\hat{\mu}_t(q^2)$ and $\hat{d}_t(q^2)$, of the top quark in the framework of the RM331, which is an economic version of the so-called 331 models with a scalar sector comprised by two scalar triplets only. We have considered the general case of an off-shell gluon as it has been pointed out before that the QCD contribution to $\hat{\mu}_t(q^2)$ is infrared divergent and the CMDM has no physical meaning for $q^2 = 0$. We argue that the results are gauge independent for $q^2 \neq 0$ and represent valid observable quantities since the structure of the gauge boson contributions are analogue to those arising in the SM. To our knowledge, no previous calculations of the off-shell CMDM and CEDM of the top quark have been presented before in the context of 331 models.

Apart from the usual SM contributions, in the RM331, the CMDM of the top quark receives new contributions from two new heavy gauge bosons Z' and V^\pm as well as one new neutral scalar boson h_2 , along with a new contribution from the neutral scalar boson h_1 , which must be identified with the 125 GeV scalar boson detected at the LHC. This model also predicts tree-level FCNCs mediated by the Z' gauge boson and the two neutral scalar bosons h_1 and h_2 , which at the one-loop level can also give rise to a non-vanishing CEDM provided that there is a CP -violating phase. The analytical results are presented in terms of both Feynman parameter integrals and Passarino-Veltman scalar functions, which are useful to cross-check the numerical results.

We present an analysis of the region of the parameter space of the model consistent with experimental data and evaluate the CMDM and CEDM of the top quark for parameter values still allowed. It is found that the new one-loop contributions of the RM331 to the real (imaginary) part of $\hat{\mu}_t(q^2)$ are of order of 10^{-5} (10^{-6}), which are larger than the predictions of other SM extensions [11], with the dominant contribution arising from the V^\pm gauge boson, whereas the remaining contributions are considerably smaller. It is also found that there is little dependence of $\mu_t(q^2)$ on $\|q\|$ in the 30-1000 GeV interval for a mass m_V of the order of a few hundreds of GeV. As far as the CEDM of the top quark is concerned, it is mainly induced by the loop with h_2 exchange and can reach values of the order of 10^{-19} for realistic values of the CP -violating phases. Such a contribution is smaller than the ones predicted by other SM extensions [11].

ACKNOWLEDGMENTS

We acknowledge support from Consejo Nacional de Ciencia y Tecnología and Sistema Nacional de Investigadores. Partial support from Vicerrectoría de Investigación y Estudios de Posgrado de la Benémrita Universidad Autónoma de Puebla is also acknowledged.

Appendix A: Feynman rules

We now present in Tables III and IV the coupling constants that enter into the Feynman rules [26, 40, 43] that follow from Eqs. (16) and (19) and are necessary for the evaluation of the CMDM and CEDM of the top quark in the RM331.

TABLE III. Coupling constants for the interactions between gauge bosons and quarks in the RM331. We follow the notation of Lagrangian (16). Here $(K_L)_{tq}$ are entries of the complex mixing matrix \mathbf{K}_L , where the subscript q runs over u and c . This matrix is given in terms of the unitary complex matrix \mathbf{V}_L^u that diagonalizes the mass matrix of up quarks, and can be written as $(K_L)_{tq} = (V_L^u)_{tq}^* (V_L^u)_{qt}$. Here $h_W = 1 - 4s_W^2$.

Coupling	$g_V^{Vqq'}$	$g_A^{Vqq'}$
$Z'\bar{t}t$	$\frac{1-2s_W^2}{2\sqrt{12}h_W}$	$\frac{1-2s_W^2}{2\sqrt{12}h_W}$
$Z\bar{t}q$	$\frac{s_W^2}{\sqrt{12}h_W} (K_L)_{tq}$	$\frac{s_W^2}{\sqrt{12}h_W} (K_L)_{tq}$
$V^-\bar{t}J_3$	$\sqrt{2}c_W (V_L^u)_{33}$	$\sqrt{2}c_W (V_L^u)_{33}$

TABLE IV. Coupling constants for the interactions between scalar bosons and quarks necessary for the evaluation of the one-loop contributions to the CMDM and CEDM in the RM331. We follow the notation of Lagrangian (19). Here $(\eta^u)_{tq}$ are entries of the complex mixing matrix $\boldsymbol{\eta}^u$, where the subscript q runs over u and c . This matrix is given in terms of the unitary complex matrices \mathbf{V}_L^u and \mathbf{V}_R^L that diagonalize the mass matrix of up quarks, and can be written as $(\eta^u)_{tq} = (V_L^u)_{tq} (V_R^u)_{qt}^*$ and $(\eta^u)_{qt}^* = (V_L^u)_{qt}^* (V_R^u)_{tq}$ since the matrix $\boldsymbol{\eta}^u$ is not symmetric.

	$G_S^{Sqq'}$	$G_P^{Sqq'}$
$h_1\bar{t}t$	$\frac{m_t}{m_W} \left(c_\beta - \frac{v_\rho}{v_\chi} s_\beta \right)$	-
$h_1\bar{t}q$	$-\frac{s_\beta v_\rho m_{33}}{v_\chi m_W} \left((\eta^u)_{tq} + (\eta^u)_{qt}^* \right)$	$-\frac{s_\beta v_\rho m_{33}}{v_\chi m_W} \left((\eta^u)_{tq} - (\eta^u)_{qt}^* \right)$
$h_2\bar{t}t$	$\frac{m_t}{m_W} \left(s_\beta - \frac{v_\rho}{v_\chi} c_\beta \right)$	-
$h_2\bar{t}q$	$\frac{c_\beta v_\rho m_{33}}{v_\chi m_W} \left((\eta^u)_{tq} + (\eta^u)_{qt}^* \right)$	$\frac{c_\beta v_\rho m_{33}}{v_\chi m_W} \left((\eta^u)_{tq} - (\eta^u)_{qt}^* \right)$

Appendix B: Analytical results for the loop integrals

In this appendix we present the loop integrals appearing in Eqs. (17), (18), (20), and (21) in terms of Feynman parameter integrals and Passarino-Veltman scalar functions both for non-zero and zero q^2 . We have verified that all the ultraviolet divergences cancel out. Furthermore, contrary to the QCD contribution, all the contribution of the RM331 are finite for $q^2 = 0$.

1. Feynman parameter integrals

The $\mathcal{V}_{qq'}^V(q^2)$ function of Eq. (17) can be written as

$$\begin{aligned} \mathcal{V}_{qq'}^V(q^2) = & \int_0^1 \int_0^{1-u} \frac{dudv}{\Delta_V} \left[2(u-1)^2 u + (1-r_{q'}) (2\hat{q}^2 uv(u+v-1) + (3u-1)\Delta_V \log(\Delta_V)) \right. \\ & \left. - r_{q'}(u-1)^2(2u-1) - (2r_{q'}^2(u-1)^2 + r_V^2 u(u+3)) + r_{q'}(r_{q'}^2(u-1)^2 - r_V^2(u-5)u) \right], \end{aligned} \quad (\text{B1})$$

where $\Delta_V = u((u-1) + r_V^2) - r_{q'}^2(u-1) + \hat{q}^2 v(u+v-1)$, with $\hat{q}^2 = q^2/m_q^2$ and $r_a = m_a/m_q$.

For $q^2 = 0$ we obtain

$$\begin{aligned} \mathcal{V}_{qq'}^V(0) = & \int_0^1 \frac{udu}{r_V^2(u-1) - u((u-1) + r_{q'}^2)} \left[u^2((1-r_{q'})^2 + 2r_V^2) - u(2r_V^2(3-2r_{q'}) + (1+r_{q'})(1-r_{q'})^2) \right. \\ & \left. + 4r_V^2(1-r_{q'}) \right]. \end{aligned} \quad (\text{B2})$$

As far as the $\tilde{\mathcal{D}}_{qq'}^V(q^2)$ function of Eq. (18) is concerned, it is given by

$$\begin{aligned} \tilde{\mathcal{D}}_{qq'}^V(q^2) = & r_{q'} \int_0^1 \int_0^{1-u} \frac{dudv}{\Delta_V} \left[(3u-1)\Delta_V \log(\Delta_V) + (2u+1)(u-1)^2 - r_{q'}^2(u-1)^2 \right. \\ & \left. + u(r_V^2(u-5) + 2\hat{q}^2 v(u+v-1)) \right], \end{aligned} \quad (\text{B3})$$

which leads to

$$\tilde{\mathcal{D}}_{qq'}^V(0) = r_{q'} \int_0^1 \frac{u(u(1-r_{q'}^2) + 4r_V^2(u-1))}{u((u-1) + r_{q'}^2) - r_V^2(u-1)} du. \quad (\text{B4})$$

The $\mathcal{P}_{qq'}^S(q^2)$ function of Eq. (20) is

$$\mathcal{P}_{qq'}^S(q^2) = \int_0^1 \int_0^{1-u} \frac{(u-1)(u-r_{q'})}{u((u-1) + r_S^2) - r_{q'}^2(u-1) + \hat{q}^2 v(u+v-1)} dudv, \quad (\text{B5})$$

which for $q^2 = 0$ simplifies to

$$\mathcal{P}_{qq'}^S(0) = \int_0^1 \frac{u^2((1-u) - r_{q'})}{u((u-1) + r_S^2) - r_{q'}^2(u-1)} du. \quad (\text{B6})$$

Finally, the loop function of Eq. (21) reads

$$\tilde{\mathcal{D}}_{qq'}^S(q^2) = \int_0^1 \int_0^{1-u} \frac{r_{q'}(u-1)}{u((u-1) + r_S^2) - r_{q'}^2(u-1) + \hat{q}^2 v(u+v-1)} dudv, \quad (\text{B7})$$

which yields

$$\tilde{\mathcal{D}}_{qq'}^S(0) = \int_0^1 \frac{r_{q'}(1-u)^2}{(1-u)(r_{q'}^2 - u) + r_S^2 u} du. \quad (\text{B8})$$

2. Passarino-Veltman results

We now present the results for the loop functions in terms of Passarino-Veltman scalar functions, which can be numerically evaluated by either LoopTools [64] or Collier [65], which allows one to cross-check the results. We introduce the following notation for the two- and three-point scalar functions in the customary notation used in the literature:

$$B_a = B_0(0, m_a^2, m_a^2), \quad (\text{B9})$$

$$B_{q'b} = B_0(m_q^2, m_{q'}^2, m_b^2), \quad (\text{B10})$$

$$B_{\hat{q}q'} = B_0(\hat{q}^2, m_{q'}^2, m_{q'}^2), \quad (\text{B11})$$

$$C_a = m_q^2 C_0(m_q^2, m_q^2, q^2, m_{q'}^2, m_a^2, m_{q'}^2). \quad (\text{B12})$$

for $a = V, S, q'$ and $b = V, S$. We also define $\delta_b = 1 - r_b$ and $\chi_b = 1 + r_b$.

For non-zero q^2 , the loop functions of Eqs. (17) and (18) are given by

$$\begin{aligned} \mathcal{V}_{qq'}^V(q^2) &= \frac{1}{(\hat{q}^2 - 4)^2} \left[(\hat{q}^2 - 4) (r_{q'}^2 - r_V^2 + 1) (\delta_{q'}^2 + 2r_V^2) + (\hat{q}^2 - 4) (\delta_{q'}^2 + 2r_V^2) (r_{q'}^2 B_{q'} - r_V^2 B_V) \right. \\ &\quad - \left(\delta_{q'}^2 \chi_{q'} ((\hat{q}^2 - 10) r_{q'} + \hat{q}^2 + 2) + r_V^2 (\hat{q}^2 (r_{q'} - 3)^2 - 2r_{q'} (5r_{q'} - 6) - 18) - 2 (\hat{q}^2 - 10) r_V^4 \right) B_{q'V} \\ &\quad + \left(\delta_{q'}^2 (2\hat{q}^2 r_{q'} - 2r_{q'} (3r_{q'} + 4) + \hat{q}^2 + 2) - 2r_V^2 (\hat{q}^2 (4r_{q'} - 5) + r_{q'} (3r_{q'} - 10) + 11) + 12r_V^4 \right) B_{\hat{q}q'} \\ &\quad + 2 \left(\delta_{q'}^3 \chi_{q'}^2 (3r_{q'} - \hat{q}^2 + 1) + \delta_{q'} r_V^2 ((5\hat{q}^2 - 8) r_{q'}^2 - (\hat{q}^2 - 4) r_{q'} - 2 ((\hat{q}^2 - 4) \hat{q}^2 + 6)) \right. \\ &\quad \left. - r_V^4 (4\hat{q}^2 (r_{q'} - 2) - (10 - 9r_{q'}) r_{q'} - 17) + 6r_V^6 \right) C_{q'V} \Big], \quad (\text{B13}) \end{aligned}$$

and

$$\tilde{\mathcal{D}}_{qq'}^V(q^2) = \frac{r_{q'}}{\hat{q}^2 - 4} \left[(r_{q'}^2 - 4r_V^2 - 1) (B_{q'V} - B_{\hat{q}q'}) + (r_V^2 (2\hat{q}^2 - 5r_{q'}^2 - 3) + (r_{q'}^2 - 1)^2 + 4r_V^4) C_{q'V} \right]. \quad (\text{B14})$$

As far as the results for $q^2 = 0$ are concerned, they read

$$\begin{aligned} \mathcal{V}_{qq'}^V(0) &= \frac{1}{r_V^2 - \chi_{q'}^2} \left[8r_V^6 - 4(r_{q'} (3r_{q'} + 2) + 2) r_V^4 + 2(r_{q'} (r_{q'} (2r_{q'} + 7) + 4) - 5) r_V^2 \right. \\ &\quad + 2(r_{q'}^2 - 1)^2 (2r_{q'} \chi_{q'} + 1) - \left(4\delta_{q'}^2 r_{q'} \chi_{q'}^3 + 4r_{q'} \chi_{q'}^2 r_V^2 - 4(r_{q'} (3r_{q'} + 2) + 3) r_V^4 + 8r_V^6 \right) B_{q'V} \\ &\quad \left. - \left(4\delta_{q'} r_{q'} \chi_{q'}^2 r_V^2 + 4(r_{q'} (r_{q'} + 2) + 3) r_V^4 - 8r_V^6 \right) B_V + 4r_{q'} (\delta_{q'}^2 \chi_{q'}^3 + r_{q'} \chi_{q'}^2 r_V^2 - 2r_{q'} r_V^4) B_{q'} \right], \quad (\text{B15}) \end{aligned}$$

and

$$\begin{aligned} \tilde{\mathcal{D}}_{qq'}^V(0) &= \frac{r_{q'}}{(1 - (r_{q'} - r_V)^2)(1 - (r_{q'} + r_V)^2)} \left[(r_{q'}^2 - r_V^2 - 1) (4r_V^4 - (5r_{q'}^2 + 3) r_V^2 + (r_{q'}^2 - 1)^2) \right. \\ &\quad + \left(4r_{q'}^2 r_V^4 + (-5r_{q'}^4 + 4r_{q'}^2 + 1) r_V^2 + (r_{q'}^2 - 1)^3 \right) B_{q'} + \left((5r_{q'}^2 + 3) r_V^4 - (r_{q'}^2 - 1)^2 r_V^2 - 4r_V^6 \right) B_V \\ &\quad \left. - \left(3(3r_{q'}^2 + 1) r_V^4 - 6r_{q'}^2 (r_{q'}^2 - 1) r_V^2 + (r_{q'}^2 - 1)^3 - 4r_V^6 \right) B_{q'V} \right]. \quad (\text{B16}) \end{aligned}$$

The loop functions of Eqs. (20) and (21) are given by

$$\begin{aligned} \mathcal{P}_{qq'}^S(q^2) &= \frac{1}{(\hat{q}^2 - 4)^2} \left[(4 - \hat{q}^2) (r_{q'}^2 - r_S^2 + 1) + (\hat{q}^2 (2r_{q'} - 1) + 6r_{q'}^2 - 8r_{q'} - 6r_S^2 - 2) B_{\hat{q}q'} \right. \\ &\quad + \left(2\delta_{q'}^2 \chi_{q'} (1 - 3r_{q'} - \hat{q}^2) + 2r_S^2 (\hat{q}^2 (r_{q'} - 2) + 6r_{q'}^2 - 4r_{q'} + 2) - 6r_S^4 \right) C_{q'S} \\ &\quad \left. + \left(\delta_{q'} ((\hat{q}^2 - 10) r_{q'} - \hat{q}^2 - 2) - (\hat{q}^2 - 10) r_S^2 \right) B_{q'S} + (\hat{q}^2 - 4) (r_S^2 B_S - r_{q'}^2 B_{q'}) \right], \quad (\text{B17}) \end{aligned}$$

and

$$\mathcal{D}_{qq'}^S(q^2) = \frac{r_{q'}}{\hat{q}^2 - 4} \left[B_{q'S} - B_{\hat{q}q'} + (r_{q'}^2 - r_S^2 - 1) C_{q'S} \right]. \quad (\text{B18})$$

For $q^2 = 0$ we obtain

$$\begin{aligned} \mathcal{P}_{qq'}^S(0) = & \frac{1}{2(\chi_{q'} - r_S)(r_{q'} + \chi_S)} \left[(4r_{q'}^2 + 2r_{q'} - 1)r_S^2 - 2r_{q'}^4 - 2r_{q'}^3 + r_{q'}^2 - 2r_S^4 - 1 \right. \\ & \left. + 2(\delta_{q'} r_{q'} \chi_{q'}^2 - r_{q'}(2r_{q'} + 1)r_S^2 + r_S^4)B_{q'S} + 2r_{q'}(r_{q'}r_S^2 - \delta_{q'}\chi_{q'}^2)B_{q'} + 2r_S^2(r_{q'}^2 + r_{q'} - r_S^2)B_S \right], \end{aligned} \quad (\text{B19})$$

and

$$\begin{aligned} \mathcal{D}_{qq'}^S(0) = & \frac{1}{(1 - (r_{q'} - r_S)^2)(1 - (r_{q'} + r_S)^2)} \left[(1 - r_{q'}^2 + r_S^2)^2 + (r_S^2(1 - r_{q'}^2 + r_S^2))(B_S - B_{q'S}) \right. \\ & \left. + (2r_S^2 - (1 - r_{q'}^2 + r_S^2)(1 - r_{q'}^2))(B_{q'S} - B_{q'}) \right]. \end{aligned} \quad (\text{B20})$$

3. Two-point scalar functions

In closing we present the closed form solutions for the two-point Passarino-Veltman scalar functions appearing in the calculation. The three-point scalar functions are too lengthy to be shown here.

$$B_0(0, m_a^2, m_a^2) = -\log\left(\frac{m_a^2}{\mu^2}\right) + \frac{1}{\epsilon} + \log(4\pi) - \gamma_E, \quad (\text{B21})$$

$$B_0(\hat{q}^2, m_{q'}^2, m_{q'}^2) = \frac{\sqrt{\hat{q}^2 - 4r_{q'}^2}}{|\hat{q}|} \log\left(\frac{|\hat{q}| \sqrt{\hat{q}^2 - 4r_{q'}^2} - \hat{q}^2 + 2r_{q'}^2}{2r_{q'}^2}\right) + 2 - \log\left(\frac{m_{q'}^2}{\mu^2}\right) + \frac{1}{\epsilon} + \log(4\pi) - \gamma_E, \quad (\text{B22})$$

$$\begin{aligned} B_0(m_q^2, m_{q'}^2, m_b^2) = & \sqrt{\lambda(x_q^2, x_b^2, x_{q'}^2)} \log\left(\frac{\sqrt{\lambda(x_q^2, x_b^2, x_{q'}^2)} + (r_b^2 + r_{q'}^2 - 1)}{2r_b r_{q'}}\right) + \frac{1}{2}(1 - r_b^2 + r_{q'}^2) \log\left(\frac{r_b^2}{r_{q'}^2}\right) \\ & + 2 - \log\left(\frac{m_b^2}{\mu^2}\right) + \frac{1}{\epsilon} + \log(4\pi) - \gamma_E, \end{aligned} \quad (\text{B23})$$

where $\lambda(x, y, z) = x^2 + y^2 + z^2 - 2(xy - xz - yz)$. The scale μ and the pole ϵ of dimensional regularization cancel out in the final result.

-
- [1] P. A. Zyla *et al.* (Particle Data Group), Review of Particle Physics, PTEP **2020**, 083C01 (2020).
[2] V. Khachatryan *et al.* (CMS), Measurements of t t-bar spin correlations and top quark polarization using dilepton final states in pp collisions at sqrt(s) = 8 TeV, Phys. Rev. D **93**, 052007 (2016), arXiv:1601.01107 [hep-ex].
[3] A. M. Sirunyan *et al.* (CMS), Search for new physics in top quark production in dilepton final states in proton-proton collisions at sqrt(s) = 13 TeV, Eur. Phys. J. C **79**, 886 (2019), arXiv:1903.11144 [hep-ex].
[4] A. M. Sirunyan *et al.* (CMS), Measurement of the top quark polarization and tt spin correlations using dilepton final states in proton-proton collisions at sqrt(s) = 13 TeV, Phys. Rev. D **100**, 072002 (2019), arXiv:1907.03729 [hep-ex].
[5] A. M. Sirunyan *et al.* (CMS), Measurement of the top quark forward-backward production asymmetry and the anomalous chromoelectric and chromomagnetic moments in pp collisions at sqrt(s) = 13 TeV, JHEP **06**, 146, arXiv:1912.09540 [hep-ex].
[6] E. P. Shabalin, Electric Dipole Moment of Quark in a Gauge Theory with Left-Handed Currents, Sov. J. Nucl. Phys. **28**, 75 (1978).
[7] A. Czarnecki and B. Krause, Neutron electric dipole moment in the standard model: Valence quark contributions, Phys. Rev. Lett. **78**, 4339 (1997), arXiv:hep-ph/9704355.
[8] I. B. Khriplovich, Quark Electric Dipole Moment and Induced θ Term in the Kobayashi-Maskawa Model, Phys. Lett. B **173**, 193 (1986).
[9] R. Martinez, M. A. Perez, and N. Poveda, Chromomagnetic Dipole Moment of the Top Quark Revisited, Eur. Phys. J. C **53**, 221 (2008), arXiv:hep-ph/0701098.
[10] I. D. Choudhury and A. Lahiri, Anomalous chromomagnetic moment of quarks, Mod. Phys. Lett. A **30**, 1550113 (2015), arXiv:1409.0073 [hep-ph].
[11] J. I. Aranda, D. Espinosa-Gómez, J. Montaño, B. Quezadas-Vivian, F. Ramírez-Zavaleta, and E. S. Tututi, Flavor violation in chromo- and electromagnetic dipole moments induced by Z' gauge bosons and a brief revisit of the Standard Model, Phys. Rev. D **98**, 116003 (2018), arXiv:1809.02817 [hep-ph].

- [12] A. I. Hernández-Juárez, A. Moyotl, and G. Tavares-Velasco, New estimate of the chromomagnetic dipole moment of quarks in the standard model, *Eur. Phys. J. Plus* **136**, 262 (2021), arXiv:2009.11955 [hep-ph].
- [13] J. I. Aranda, T. Cisneros-Pérez, J. Montaña, B. Quezadas-Vivian, F. Ramírez-Zavaleta, and E. S. Tututi, Revisiting the top quark chromomagnetic dipole moment in the SM, *Eur. Phys. J. Plus* **136**, 164 (2021), arXiv:2009.05195 [hep-ph].
- [14] R. Gaitan, E. A. Garces, J. H. M. de Oca, and R. Martinez, Top quark Chromoelectric and Chromomagnetic Dipole Moments in a Two Higgs Doublet Model with CP violation, *Phys. Rev. D* **92**, 094025 (2015), arXiv:1505.04168 [hep-ph].
- [15] A. I. Hernández-Juárez, A. Moyotl, and G. Tavares-Velasco, Chromomagnetic and chromoelectric dipole moments of the top quark in the fourth-generation THDM, *Phys. Rev. D* **98**, 035040 (2018), arXiv:1805.00615 [hep-ph].
- [16] Q.-H. Cao, C.-R. Chen, F. Larios, and C. P. Yuan, Anomalous gtt couplings in the Littlest Higgs Model with T-parity, *Phys. Rev. D* **79**, 015004 (2009), arXiv:0801.2998 [hep-ph].
- [17] L. Ding and C.-X. Yue, Top quark chromomagnetic dipole moment in the littlest Higgs model with T-parity, *Commun. Theor. Phys.* **50**, 441 (2008), arXiv:0801.1880 [hep-ph].
- [18] A. Aboubrahim, T. Ibrahim, P. Nath, and A. Zorik, Chromoelectric Dipole Moments of Quarks in MSSM Extensions, *Phys. Rev. D* **92**, 035013 (2015), arXiv:1507.02668 [hep-ph].
- [19] R. Martinez, M. A. Perez, and O. A. Sampayo, Constraints on unparticle physics from the $gt\bar{t}$ anomalous coupling, *Int. J. Mod. Phys. A* **25**, 1061 (2010), arXiv:0805.0371 [hep-ph].
- [20] T. Ibrahim and P. Nath, The Chromoelectric Dipole Moment of the Top Quark in Models with Vector Like Multiplets, *Phys. Rev. D* **84**, 015003 (2011), arXiv:1104.3851 [hep-ph].
- [21] J. G. Ferreira, Jr, P. R. D. Pinheiro, C. A. d. S. Pires, and P. S. R. da Silva, The Minimal 3-3-1 model with only two Higgs triplets, *Phys. Rev. D* **84**, 095019 (2011), arXiv:1109.0031 [hep-ph].
- [22] B. W. Lee and S. Weinberg, $SU(3) \times U(1)$ Gauge Theory of the Weak and Electromagnetic Interactions, *Phys. Rev. Lett.* **38**, 1237 (1977).
- [23] F. Pisano and V. Pleitez, An $SU(3) \times U(1)$ model for electroweak interactions, *Phys. Rev. D* **46**, 410 (1992), arXiv:hep-ph/9206242.
- [24] P. H. Frampton, Chiral dilepton model and the flavor question, *Phys. Rev. Lett.* **69**, 2889 (1992).
- [25] J. D. Ruiz-Alvarez, C. A. de S. Pires, F. S. Queiroz, D. Restrepo, and P. S. Rodrigues da Silva, On the Connection of Gamma-Rays, Dark Matter and Higgs Searches at LHC, *Phys. Rev. D* **86**, 075011 (2012), arXiv:1206.5779 [hep-ph].
- [26] C. Kelso, C. A. de S. Pires, S. Profumo, F. S. Queiroz, and P. S. Rodrigues da Silva, A 331 WIMPy Dark Radiation Model, *Eur. Phys. J. C* **74**, 2797 (2014), arXiv:1308.6630 [hep-ph].
- [27] E. Ramirez Barreto, Y. A. Coutinho, and J. Sa Borges, Vector- and Scalar-Bilepton Pair Production in Hadron Colliders, *Phys. Rev. D* **83**, 075001 (2011), arXiv:1103.1267 [hep-ph].
- [28] E. Ramirez Barreto, Y. A. Coutinho, and J. Sa Borges, Searching for an Extra Neutral Gauge Boson from Muon Pair Production at LHC, *Phys. Lett. B* **689**, 36 (2010), arXiv:1004.3269 [hep-ph].
- [29] E. Ramirez Barreto, Y. A. Coutinho, and J. Sa Borges, Charged Bilepton Pair Production at LHC Including Exotic Quark Contribution, *Nucl. Phys. B* **810**, 210 (2009), arXiv:0811.0846 [hep-ph].
- [30] V. Q. Phong, V. T. Van, and H. N. Long, Electroweak phase transition in the reduced minimal 3-3-1 model, *Phys. Rev. D* **88**, 096009 (2013), arXiv:1309.0355 [hep-ph].
- [31] P. V. Dong, N. T. K. Ngan, and D. V. Soa, Simple 3-3-1 model and implication for dark matter, *Phys. Rev. D* **90**, 075019 (2014), arXiv:1407.3839 [hep-ph].
- [32] A. Das, K. Enomoto, S. Kanemura, and K. Yagyu, Radiative generation of neutrino masses in a 3-3-1 type model, *Phys. Rev. D* **101**, 095007 (2020), arXiv:2003.05857 [hep-ph].
- [33] D. Cogollo, H. Diniz, C. A. de S. Pires, and P. S. Rodrigues da Silva, The Seesaw mechanism at TeV scale in the 3-3-1 model with right-handed neutrinos, *Eur. Phys. J. C* **58**, 455 (2008), arXiv:0806.3087 [hep-ph].
- [34] F. Queiroz, C. A. de S. Pires, and P. S. R. da Silva, A minimal 3-3-1 model with naturally sub-eV neutrinos, *Phys. Rev. D* **82**, 065018 (2010), arXiv:1003.1270 [hep-ph].
- [35] W. Caetano, C. A. de S. Pires, P. S. Rodrigues da Silva, D. Cogollo, and F. S. Queiroz, Explaining ATLAS and CMS Results Within the Reduced Minimal 3-3-1 model, *Eur. Phys. J. C* **73**, 2607 (2013), arXiv:1305.7246 [hep-ph].
- [36] A. G. Dias, P. R. D. Pinheiro, C. A. de S. Pires, and P. S. Rodrigues da Silva, A compact 341 model at TeV scale, *Annals Phys.* **349**, 232 (2014), arXiv:1309.6644 [hep-ph].
- [37] J. G. Ferreira, C. A. de S. Pires, P. S. Rodrigues da Silva, and A. Sampieri, Higgs sector of the supersymmetric reduced 331 model, *Phys. Rev. D* **88**, 105013 (2013), arXiv:1308.0575 [hep-ph].
- [38] V. V. Vien and H. N. Long, The D_4 flavor symmetry in 3-3-1 model with neutral leptons, *Int. J. Mod. Phys. A* **28**, 1350159 (2013), arXiv:1312.5034 [hep-ph].
- [39] V. T. N. Huyen, H. N. Long, T. T. Lam, and V. Q. Phong, Neutral Current in Reduced Minimal 3-3-1 Model, *Commun. in Phys.* **24**, 97 (2014), arXiv:1210.5833 [hep-ph].
- [40] D. Cogollo, F. S. Queiroz, and P. Vasconcelos, Flavor Changing Neutral Current Processes in a Reduced Minimal Scalar Sector, *Mod. Phys. Lett. A* **29**, 1450173 (2014), arXiv:1312.0304 [hep-ph].
- [41] C. Kelso, H. N. Long, R. Martinez, and F. S. Queiroz, Connection of $g - 2_\mu$, electroweak, dark matter, and collider constraints on 331 models, *Phys. Rev. D* **90**, 113011 (2014), arXiv:1408.6203 [hep-ph].
- [42] G. De Conto and V. Pleitez, Electron and muon anomalous magnetic dipole moment in a 3-3-1 model, *JHEP* **05**, 104, arXiv:1603.09691 [hep-ph].
- [43] A. C. B. Machado, J. C. Montero, and V. Pleitez, Flavor-changing neutral currents in the minimal 3-3-1 model revisited, *Phys. Rev. D* **88**, 113002 (2013), arXiv:1305.1921 [hep-ph].

- [44] S. Tatur and J. Bartelski, Mass matrices for quarks and leptons in triangular form, *Acta Phys. Polon. B* **39**, 2903 (2008), arXiv:0801.0095 [hep-ph].
- [45] D. Binosi and J. Papavassiliou, Pinch Technique: Theory and Applications, *Phys. Rept.* **479**, 1 (2009), arXiv:0909.2536 [hep-ph].
- [46] A. Denner, G. Weiglein, and S. Dittmaier, Application of the background field method to the electroweak standard model, *Nucl. Phys. B* **440**, 95 (1995), arXiv:hep-ph/9410338.
- [47] V. Shtabovenko, R. Mertig, and F. Orellana, New Developments in FeynCalc 9.0, *Comput. Phys. Commun.* **207**, 432 (2016), arXiv:1601.01167 [hep-ph].
- [48] H. H. Patel, Package-X: A Mathematica package for the analytic calculation of one-loop integrals, *Comput. Phys. Commun.* **197**, 276 (2015), arXiv:1503.01469 [hep-ph].
- [49] G. Aad *et al.* (ATLAS), Search for a heavy charged boson in events with a charged lepton and missing transverse momentum from pp collisions at $\sqrt{s} = 13$ TeV with the ATLAS detector, *Phys. Rev. D* **100**, 052013 (2019), arXiv:1906.05609 [hep-ex].
- [50] A. M. Sirunyan *et al.* (CMS), Search for high-mass resonances in final states with a lepton and missing transverse momentum at $\sqrt{s} = 13$ TeV, *JHEP* **06**, 128, arXiv:1803.11133 [hep-ex].
- [51] G. Aad *et al.* (ATLAS), Search for new resonances in mass distributions of jet pairs using 139 fb^{-1} of pp collisions at $\sqrt{s} = 13$ TeV with the ATLAS detector, *JHEP* **03**, 145, arXiv:1910.08447 [hep-ex].
- [52] A. M. Sirunyan *et al.* (CMS), Search for high mass dijet resonances with a new background prediction method in proton-proton collisions at $\sqrt{s} = 13$ TeV, *JHEP* **05**, 033, arXiv:1911.03947 [hep-ex].
- [53] G. Aad *et al.* (ATLAS), Search for high-mass dilepton resonances using 139 fb^{-1} of pp collision data collected at $\sqrt{s} = 13$ TeV with the ATLAS detector, *Phys. Lett. B* **796**, 68 (2019), arXiv:1903.06248 [hep-ex].
- [54] A. M. Sirunyan *et al.* (CMS), Search for resonant and nonresonant new phenomena in high-mass dilepton final states at $\sqrt{s} = 13$ TeV, (2021), arXiv:2103.02708 [hep-ex].
- [55] E. R. Barreto, A. G. Dias, J. Leite, C. C. Nishi, R. L. N. Oliveira, and W. C. Vieira, Hierarchical fermions and detectable Z' from effective two-Higgs-triplet 3-3-1 model, *Phys. Rev. D* **97**, 055047 (2018), arXiv:1709.09946 [hep-ph].
- [56] H. N. Long, N. V. Hop, L. T. Hue, and N. T. T. Van, Constraining heavy neutral gauge boson Z' in the 3 - 3 - 1 models by weak charge data of Cesium and proton, *Nucl. Phys. B* **943**, 114629 (2019), arXiv:1812.08669 [hep-ph].
- [57] H. N. Long, N. V. Hop, L. T. Hue, N. H. Thao, and A. E. Cárcamo Hernández, Some phenomenological aspects of the 3-3-1 model with the Cárcamo-Kovalenko-Schmidt mechanism, *Phys. Rev. D* **100**, 015004 (2019), arXiv:1810.00605 [hep-ph].
- [58] A. M. Sirunyan *et al.* (CMS), Search for vector-like quarks in events with two oppositely charged leptons and jets in proton-proton collisions at $\sqrt{s} = 13$ TeV, *Eur. Phys. J. C* **79**, 364 (2019), arXiv:1812.09768 [hep-ex].
- [59] A. M. Sirunyan *et al.* (CMS), Search for single production of vector-like quarks decaying to a top quark and a W boson in proton-proton collisions at $\sqrt{s} = 13$ TeV, *Eur. Phys. J. C* **79**, 90 (2019), arXiv:1809.08597 [hep-ex].
- [60] M. Aaboud *et al.* (ATLAS), Search for pair production of heavy vector-like quarks decaying into high- p_T W bosons and top quarks in the lepton-plus-jets final state in pp collisions at $\sqrt{s} = 13$ TeV with the ATLAS detector, *JHEP* **08**, 048, arXiv:1806.01762 [hep-ex].
- [61] S. Tatur and J. Bartelski, Triangular mass matrices for quarks and leptons, *Phys. Rev. D* **74**, 013007 (2006), arXiv:hep-ph/0605261.
- [62] E. O. Iltan, Top quark electric and chromo electric dipole moments in the general two Higgs doublet model, *Phys. Rev. D* **65**, 073013 (2002), arXiv:hep-ph/0111038.
- [63] D. Atwood, S. Bar-Shalom, G. Eilam, and A. Soni, CP violation in top physics, *Phys. Rept.* **347**, 1 (2001), arXiv:hep-ph/0006032.
- [64] T. Hahn and M. Perez-Victoria, Automatized one loop calculations in four-dimensions and D-dimensions, *Comput. Phys. Commun.* **118**, 153 (1999), arXiv:hep-ph/9807565.
- [65] A. Denner, S. Dittmaier, and L. Hofer, Collier: a fortran-based Complex One-Loop Library in Extended Regularizations, *Comput. Phys. Commun.* **212**, 220 (2017), arXiv:1604.06792 [hep-ph].